Journal of Physics: Conference Series **487** (2014) 012005 doi:10.1088/1742-6596/487/1/012005

Bicritical or tetracritical: the 3D anisotropic Heisenberg antiferromagnet

Shan-Ho Tsai[1,2], Siyan Hu[1], and D. P. Landau[1]

[1] Center for Simulational Physics, University of Georgia, Athens, GA 30602, USA
[2] Georgia Advanced Computing Resource Center, Enterprise Information Technology Services, University of Georgia, Athens, GA 30602, USA

E-mail: shtsai@uga.edu

Abstract.
The classical uniaxially anisotropic Heisenberg antiferromagnet on the simple cubic lattice, in the presence of an external magnetic field, is believed to have a multicritical point; however, there has been controversy whether it is a bicritical or a tetracritical point. We perform Monte Carlo simulations of this model and analyze the components of the staggered magnetization, the susceptibilities and the probability distribution of the magnetization to conclude that the multicritical point is bicritical and it is in the three-dimensional Heisenberg universality class.

1. Introduction

The Hamiltonian of the uniaxially anisotropic Heisenberg antiferromagnetic model is given by:

$$\mathcal{H} = J \sum_{\langle i,j \rangle} [\Delta(S_i^x S_j^x + S_i^y S_j^y) + S_i^z S_j^z] - H \sum_{i=1}^{N} S_i^z \tag{1}$$

where the three-component unit vectors $\mathbf{S}_i = (S_i^x, S_i^y, S_i^z)$ represent classical spins on sites i of a simple cubic lattice, with linear size L, and $J > 0$ is the exchange coupling between nearest-neighbor pairs of spins. The first summation is over all $\langle i, j \rangle$ pairs of neighboring sites and the second summation is over all $N = L^3$ lattice sites. The uniaxial exchange anisotropy Δ is set to $\Delta = 0.8$, which gives rise to an easy axis in the z direction. A magnetic field H is applied along the $z-$axis. This model is also referred to as the XXZ antiferromagnet and it provides a good description of many real magnetic systems, including $NiCl_2 6H_2O$ [1, 2, 3], MnF_2 [4, 5, 6], and $GdAlO_3$ [7, 8, 9], among others. A different anisotropic Heisenberg model, which has a crystal field term, is studied in Ref.[10].

Early leading-order renormalization group theory [11], Monte Carlo simulations [12], high-temperature series expansion [13], among other studies, concluded that the model described above has an antiferromagnetic (AF) phase (see Fig. 1(a)) at low temperature T and low field H, a spin-flop (SF) phase (see Fig. 1(b)) at low T and higher H, and a paramagnetic (P) phase at high T and/or at high H. The AF to P phase transition line is in the Ising universality class, while the SF to P phase transition line is in the XY universality class in this picture. The AF and SF phases are separated by a first-order phase transition line and the three phases meet at a bicritical point, which is in the three-dimensional (3D) Heisenberg universality class. Later, a

renormalization group theory in higher-loop order [14] finds the presence of a tetracritical point for this model with a new biconical phase (see Fig. 1(c)). A subsequent renormalization group study in two-loop order proposes that a bicritical point in the 3D Heisenberg universality class cannot be excluded [15]. Recent Monte Carlo simulations using Metropolis sampling, focusing on simple cubic lattices with linear sizes L up to 32, and carrying out critical property analysis using finite size scaling on the multicritical point [16, 17] corroborate a scenario with a bicritical point in the 3D Heisenberg universality class. However, a subsequent numerical analysis of anisotropic perturbations in three-dimensional O(N)-symmetric vector models suggests [18] that for the model in question here, the stable fixed point has a biconical structure (see Fig. 1(c)), and its critical exponents are very close to the ones in the 3D Heisenberg universality class [19]. Therefore, it is very hard to distinguish between a bicritical point in the Heisenberg universality class and a tetracritical point (with a biconical phase) using Monte Carlo simulations and finite-size scaling to determine critical exponents at the multicritical point. Figure 2 shows a schematic view of the different phase diagrams that have been proposed for this model.

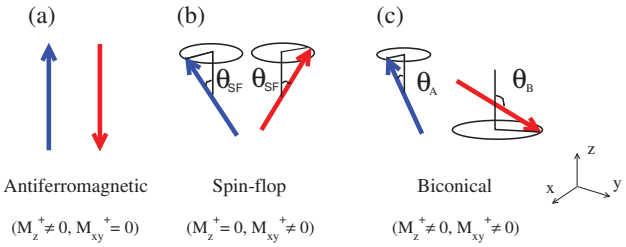

Figure 1. Illustration of spin configurations of the sublattices in the antiferromagnetic, spin-flop, and biconical phases.

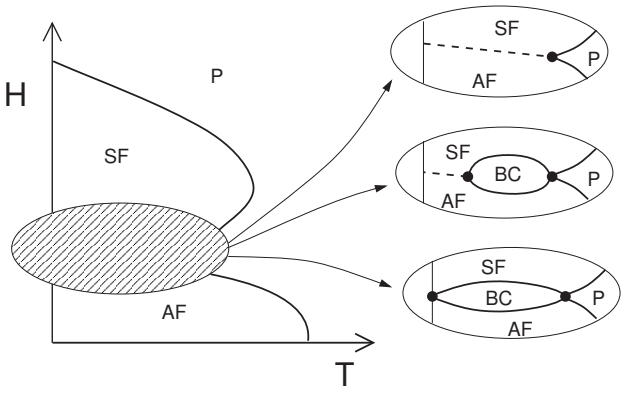

Figure 2. Schematic plot of the phase diagram with the three suggested scenarios for the region near the multicritical point. AF, SF, BC, and P label an antiferromagnetic, a spin-flop, a biconical, and a paramagnetic phase, respectively.

In this paper we use Monte Carlo simulations with a hybrid sampling method that includes Metropolis and Wolff-cluster steps, and use larger lattices to determine the nature of the multicritical point. Instead of obtaining critical exponents at the multicritical point, we examine the order of the AF to SF phase transition below, but near, the multicritical point and investigate whether a biconical phase is present. We also compare the probability distribution of the uniform magnetization, which is a universal quantity, with the distribution of the 3D Heisenberg universality class.

2. Simulation methods

We carried out Monte Carlo simulations [20] for the model described in Eq.(1) using a hybrid method that consists of Metropolis single-spin-flip sampling [21], combined with the Wolff-cluster algorithm [22] applied to the z-component of the spins, i.e. S_i^z. A typical run consists of $10^7 \sim 1.5 \times 10^8$ hybrid Monte Carlo steps (MCS), where each hybrid Monte Carlo step consists

of 6 Wolff-cluster steps and 4 sweeps through the lattice using Metropolis sampling. The Wolff-cluster algorithm implemented here satisfies detailed balance, but it is not ergodic, because it only changes the z component of the spins ; however, the hybrid sampling method used here is ergodic and it satisfies detailed balance. This hybrid sampling method allowed us to use larger lattice sizes, with linear dimensions $10 \leq L \leq 60$. Periodic boundary conditions are used to minimize finite size effects. We also use histogram reweighting methods [23] to obtain results for temperatures and external fields near the values at which simulations were performed. Several independent runs were carried out to compute error bars in the quantities; whenever error bars are not shown in the figures, they are of the size of or smaller than the symbol sizes.

In order to determine the phase transition line between the AF and SF phases and to detect a possible biconical phase, we examine the components of the staggered magnetization along the z direction and on the xy plane, *i.e.* M_z^+ and M_{xy}^+, respectively. These quantities are defined by

$$M_z^+ = |M_{z,A} - M_{z,B}| \tag{2}$$

$$M_{xy}^+ = \sqrt{(M_{x,A} - M_{x,B})^2 + (M_{y,A} - M_{y,B})^2} \tag{3}$$

where $(M_{x,i}, M_{y,i}, M_{z,i})$ are the x, y, and z components of the uniform magnetization on sublattices $i = A, B$. In the AF phase, M_z^+ is non-zero and M_{xy}^+ is zero, whereas in the SF phase M_z^+ vanishes but M_{xy}^+ does not. Therefore these two quantities can be used as order parameters for the phase transitions between the AF and SF phases. A concurrent, non-zero value of M_z^+ and M_{xy}^+ would reveal a biconical phase. The susceptibilities χ_{xy}^+ and χ_z^+ are computed from the fluctuations of M_{xy}^+ and M_z^+, respectively. To simplify notation, we set $J = 1$ and the Boltzmann constant $k_B = 1$.

3. Results

The phase diagram for the XXZ model described by the Hamiltonian in Eq. (1), as obtained by Selke [17], is shown in Fig. 1 of Ref.[17]. The multicritical point where the AF, SF, and P phases meet was determined to be [17] at $k_BT/J = 1.025 \pm 0.0025$ and $H/J = 3.89 \pm 0.01$.

Below the multicritical point, if we fix the temperature T and vary the external field H from the AF to the SF phase, we would see a single first-order phase transition point in the absence of a biconical phase. If a biconical phase exists, then two second-order phase transition points, separating the AF and BC phases and the BC and SF phases, would be seen.

At $T = 0.95$ the ensemble average of the order parameters M_{xy}^+ and M_z^+ per site as a function of H, shown in Fig. 3, indicate that a single phase transition occurs around $H = 3.8382$ (shown by the dashed line in Fig. 3). The peak positions of the susceptibilities χ_{xy}^+ and χ_z^+ (see Fig. 4) occur at the same field (marked by dashed line in Fig. 4), which corroborates that a single phase transition between the AF and the SF phase occurs at this temperature. Hence, we see no evidence of a biconical phase at $T = 0.95$.

Next, we consider a temperature closer to the multicritical point, namely $T = 0.98$. Fig. 5 shows the ensemble average of the order parameters M_{xy}^+ and M_z^+ per site as a function of H at $T = 0.98$. Again, the curves for the larger lattice sizes show that a single phase transition happens around $H = 3.8614$ (shown by the dashed line in Fig. 5). The presence of a single phase transition is confirmed by the location of the peaks in χ_{xy}^+ and χ_z^+, which occur at the same field (shown by the dashed line in Fig. 6). We have also plotted the order parameters and their susceptibilities at $T = 1.01$ (results not shown here), and we have seen no evidence of a biconical phase.

The order of the AF to SF phase transition points at temperatures below the multicritical point is determined with a finite-size scaling plot of the logarithm of the maximum of the susceptibilities χ_{xy}^+ and χ_z^+ as a function of L. For a first-order phase transition, the maximum

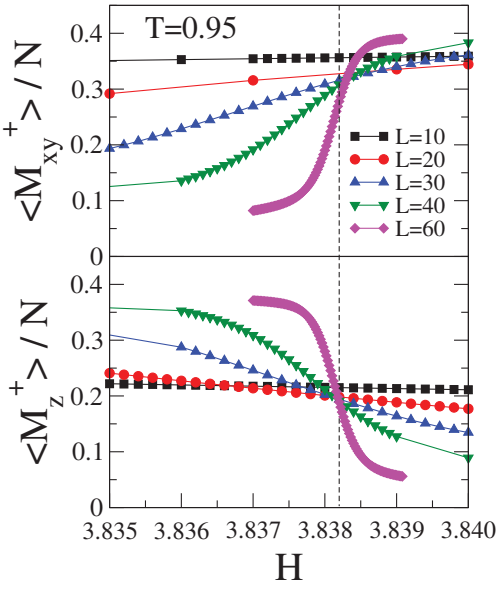

Figure 3. Components of the staggered magnetization per site as a function of H for $T = 0.95$. The dashed line marks $H = 3.8382$.

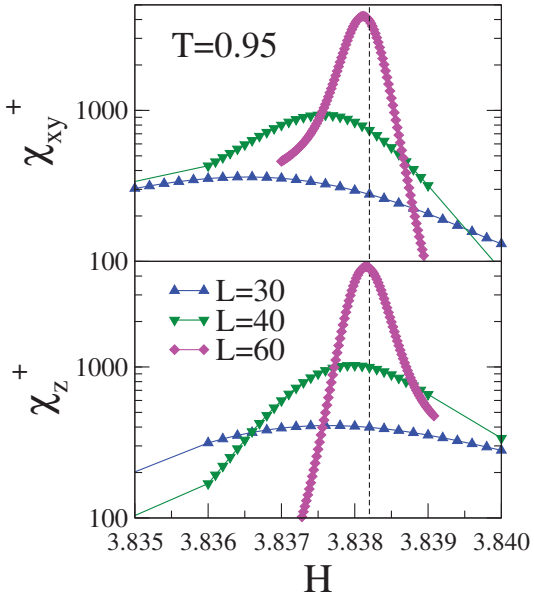

Figure 4. Magnetic susceptibilities χ^+_{xy} and χ^+_z as a function of the external field H for $T = 0.95$. The dashed line marks $H = 3.8382$.

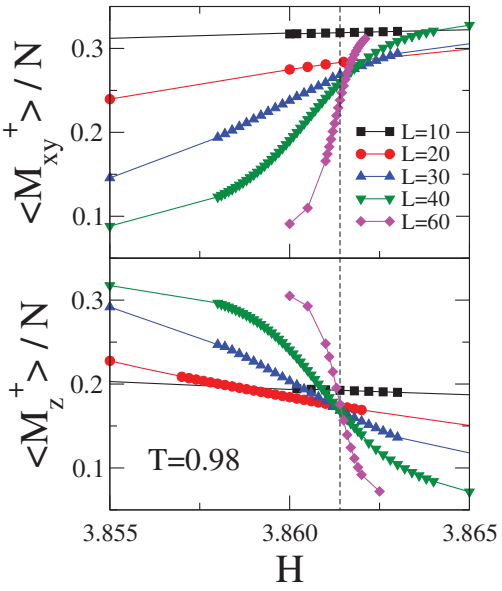

Figure 5. Components of the staggered magnetization per site as a function of H for $T = 0.98$. The dashed line marks $H = 3.8614$.

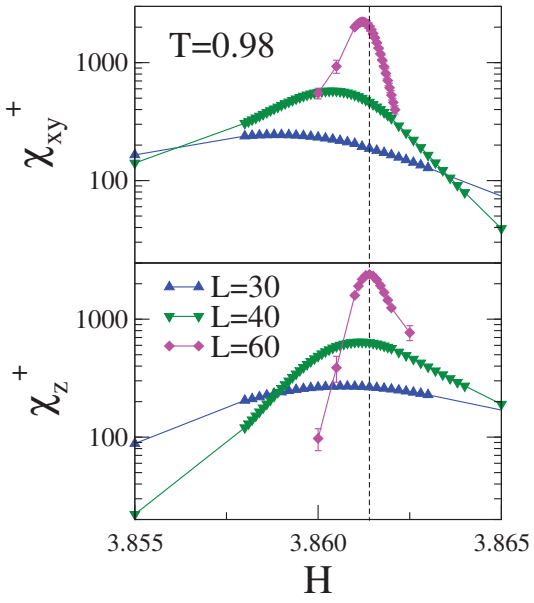

Figure 6. Magnetic susceptibilities χ^+_{xy} and χ^+_z as a function of external field H for $T = 0.98$. The dashed line marks $H = 3.8614$.

of the susceptibility of the order parameter scales as L^d, where d is the dimension of the lattice. Linear least-squares fitting of the maximum of χ^+_{xy} and χ^+_z as a function of L in a log-log plot

(see Figs. 7(a) and 7(b)) show that the slopes in these graphs are very close to 3, which is the dimension of the simple cubic lattice used here. For $T = 1.01$, due to the proximity to the multicritical point, the linear fitting gives a slope close to 3 when the smaller lattices ($L = 10, 20$) are excluded from the fitting. These results indicate that the AF to SF phase transition points at these temperatures below, but quite near, the multicritical point are of first order.

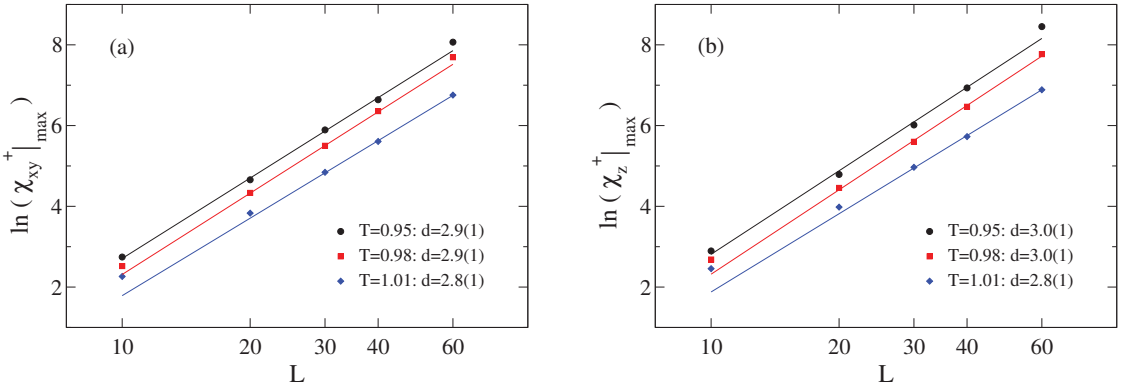

Figure 7. Logarithm of the maximum of the susceptibilities (a) χ^+_{xy} and (b) χ^+_z as a function of L for temperatures below the multicritical point. The linear fitting for $T = 0.95$, $T = 0.98$, and $T = 1.01$ includes data points for $L = 10$ to 60, $L = 20$ to 60, and $L = 30$ to 60, respectively.

In order to determine the nature of the multicritical point, we consider the universal scaling function $P^*(m/\sigma)$, where σ is the variance of the uniform magnetization $m = \sqrt{M_x^2 + M_y^2 + M_z^2}$, which we rescale to m/σ. The probability distribution has the following form [25, 26]:

$$P(m) = \frac{1}{\sigma} P^*(m/\sigma) \tag{4}$$

where σ is calculated as $\sigma^2 = < m^2 > - < m >^2$. Fig. 8 shows the comparison of our probability distribution for $L = 30$ and $L = 40$ with the probability distribution for the $3D$ Heisenberg model. We used histogram reweighting in T and H to obtain curves that best match the $3D$ Heisenberg probability distribution. The distribution for the Heisenberg model was obtained for $L = 40$, at the critical point [24]. These unit-variance, zero-average curves collapse very nicely; hence, we have confidence in concluding that the meeting point of the AF, SF, and P phases belongs to the $3D$ Heisenberg universality class.

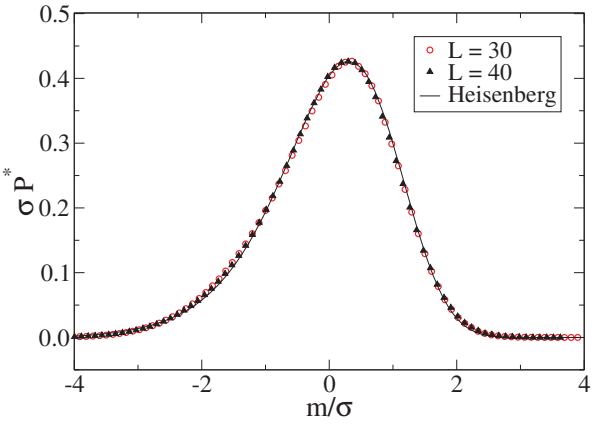

Figure 8. Scaling function $P^*(m/\sigma)$ for $L = 30$ and $L = 40$ at the multicritical point, and for the 3D Heisenberg model at its critical point.

4. Conclusions

Monte Carlo simulations with Wolff-cluster and Metropolis sampling methods are used to study the uniaxially anisotropic Heisenberg antiferromagnet (XXZ model) in an external field H along the z direction, on simple cubic lattices. By looking at fixed temperatures $T = 0.95$, $T = 0.98$, and $T = 1.01$ below the multicritical point, we determined that for each T there is a single first-order phase transition between the antiferromagnetic and the spin-flop phases. We have seen no evidence of a biconical phase. Because the critical exponents at a tetracritical point are very close to those at a bicritical point in the 3D Heisenberg universality class, it is very hard to use critical exponent values to determine the nature of the multicritical point. Hence, we used the probability distribution of the magnetization for this purpose. An excellent collapse of this probability distribution with the universal distribution of the $3D$ Heisenberg model leads us to conclude that the multicritical point in the XXZ model is indeed a bicritical point in the $3D$ Heisenberg universality class.

Acknowledgments

We are grateful to J. A. Plascak for very helpful discussions. This work was supported by NSF Grant number DMR-0810223 and it was supported in part by resources from the Georgia Advanced Computing Resource Center, a partnership between the University of Georgia's Office of the Vice President for Research and Office of the Vice President for Information Technology.

References

[1] Oliveira Jr N F, Paduan Filho A, Salinas S R 1975 *Phys. Lett.* A **55** 293
[2] Oliveira Jr N F, Paduan Filho A, Salinas S R 1976 *AIP Conf. Proc.* **29** 463
[3] Oliveira Jr N F, Paduan Filho A, Salinas S R and Becerra C C 1978 *Phys. Rev.* B **18** 6165
[4] Shapira Y and Foner S 1970 *Phys. Rev.* B **1** 3083
[5] King A R and Rohrer H 1976 *AIP Conf. Proc.* **29** 420
[6] Shapira Y and Becerra C C 1976 *Phys. Lett.* A **57** 483
[7] Rohrer H 1975 *Phys. Rev. Lett.* **34** 1638
[8] Rohrer H 1975 *AIP Conf. Proc.* **24** 268
[9] Rohrer H and Gerber Ch 1977 *Phys. Rev. Lett.* **38** 909
[10] Freire R T S, Martins P H L and Plascak J A *Journal of Physics Conference Series* current volume
[11] Nelson D R, Kosterlitz J M and Fisher M E 1974 *Phys. Rev. Lett.* **33** 813
[12] Landau D P and Binder K 1978 *Phys. Rev.* B **17** 2328
[13] Mouritsen O G, Kjaersgaard Hansen E and Knak Jensen S J 1980 *Phys. Rev.* B **22** 3256
[14] Calabrese P, Pelissetto A and Vicari E 2003 *Phys. Rev.* B **67** 054505
[15] Folk R, Holovatch Y and Moser G 2008 *Phys. Rev.* E **78** 041124
[16] Bannasch G and Selke W 2009 *Euro. Phys. J.* B **69** 439
[17] Selke W 2011 *Phys. Rev.* E **83** 042102
[18] Hasenbusch M and Vicari E 2011 *Phys. Rev.* B **84** 125136
[19] Campostrini M, Hasenbusch M, Pelissetto A, Rossi P and Vicari E 2002 *Phys. Rev.* B **65** 144520
[20] Landau D P and Binder K 2009 *A Guide to Monte Carlo Simulations in Statistical Physics* (Cambridge: Cambridge University Press)
[21] Metropolis N, Rosenbluth A W, Rosenbluth M N, Teller A H and Teller E 1953 *J. Chem. Phys.* **21** 1087
[22] Wolff U 1989 *Phys. Rev. Lett.* **62** 361
[23] Ferrenberg A M and Swendsen R H 1988 *Phys. Rev. Lett.* **61** 2635
[24] Chen K, Ferrenberg A M and Landau D P 1993 *Phys. Rev.* B **48** 3249
[25] Martins P H L and Plascak J A 2007 *Phys. Rev.* E **76** 012102
[26] Plascak J A and Martins P H L 2013 *Comp. Phys. Comm.* **184** 259